Chapter 37

Methods for the Detection of DNA Damage

D.V. Firsanov[1,2], L.V. Solovjeva[1], V.M. Mikhailov[1], M.P. Svetlova[1]

[1]Institute of Cytology of the Russian Academy of Sciences, Saint-Petersburg, Russia; [2]Nikiforov Russian Center of Emergency and Radiation Medicine of the EMERCOM of Russia, Saint-Petersburg, Russia

Chapter Outline

1. INTRODUCTION

The sources of cellular DNA damage can be endogenous or exogenous. Among a variety of exogenous factors causing DNA damage, UV radiation from the sun, environmental chemicals, and ionizing radiation (IR) that can come from natural sources and medical procedures are well known. Endogenous sources of DNA damage are associated mainly with reactive oxygen species (ROS) production during normal cellular metabolism. The damage can be induced both in nuclear and mitochondrial DNA.

Abasic sites (AP sites) appear in DNA as a result of spontaneous hydrolysis of N-glycosidic bonds or the action of DNA glycosylases, whereas ROS leads to the induction of 7,8-dihydro-8-oxogunine (8-oxo-guanine), formamidopyrimidines, ring-saturated pyrimidines such as thymine glycols, and single-strand breaks (SSBs) or double-strand breaks (DSBs) in DNA [1,2].

IR-induced DNA damages include oxidized bases, DSBs, and SSBs: the latter are a predominant form of lesions produced by IR. DSBs are considered to be the most toxic form of DNA damage of living cells. DSBs can also arise after the action of some radiomimetic drugs like bleomycin or the inhibition of topoisomerase reaction.

Two main types of DNA lesions are generated after UV light exposure—cyclobutane pyrimidine dimers (CPD) and pyrimidine (6-4) pyrimidone photoproducts (6-4PP)—that bend the DNA molecule and interfere with DNA replication and transcription [3,4].

Genome Stability. http://dx.doi.org/10.1016/B978-0-12-803309-8.00037-9

Cellular DNA can also be damaged by chemical agents, some of which cause cancer. Chemical carcinogens are classified into two categories: direct- and indirect-acting. Direct-acting carcinogens such as nitrogen mustard, methyl nitrosourea, and dimethyl sulfate react with DNA themselves. Indirect-acting carcinogens such as benzo[a]pyrene, 2-acethylaminofluorene, and 2-naphtylamine must be metabolized before they can react with DNA. Indirect-acting carcinogens can modify DNA bases, forming DNA adducts only after conversion carried out by certain enzymes. DNA adducts lead to the incorporation of incorrect bases in daughter DNA strands during replication and the appearance of new mutations. Mutations in particular genes can induce cancer. For example, different types of cancer show a high incidence of p53 protein mutations that are associated with the loss of wild-type p53 tumor-suppression activity and contribute to malignant transformations [5].

Besides cancer, DNA lesions can lead to other deleterious biological consequences. The accumulation of DNA damage occurs during normal human aging. The development of hereditary diseases associated with the accelerated aging, such as ataxia telangiectasia, Bloom syndrome, Fanconi anemia, and others, is caused by mutations in certain genes.

A number of DNA repair protein systems are activated during cellular DNA damage response (DDR). DNA repair enzymes correct the structure of DNA, prevent the formation of mutations, and maintain DNA integrity.

Single damaged nucleotide bases that arise during DNA oxidation or the action of chemical mutagens on DNA are removed by base excision repair (BER) (see review [6]). BER includes the following steps: the recognition and removal of damaged bases by DNA glycosylase forming apurinic/apyrimidinic sites also known as abasic (AP) sites, the incision of AP site with AP endonuclease, the elimination of a sugar fragment by a phosphodiesterase, repair synthesis by DNA polymerase, and end ligation. A number of different DNA glycosylases that target deaminated, alkylated, and oxidized bases are described.

UV-induced lesions, CPDs and 6-4PPs, are repaired by nucleotide excision repair (NER). More than 30 proteins participate in this type of repair. NER eliminates a broad range of damages including not only CPDs and 6-4PPs but bulky chemical adducts and some forms of oxidative damage. Two sub-pathways of NER, global genomic repair (GGR) and transcription-coupled repair (TCR), are known (reviewed in Refs. [7,8]). Four steps of NER include: the detection of damage, excision of DNA fragment containing a lesion, gap filling with DNA polymerase, and ligation of DNA ends. The main proteins involved in NER include XPA, XPB, XPC, XPD, XPE, XPF, XPG, CSA, and CSB. Mutations in NER proteins are responsible for hereditary diseases such as xeroderma pigmentosum (XP proteins), and Cockayne syndrome (CSA and CSB proteins). TCR and GGR differ in the first step of repair. TCR is initiated when RNA polymerase stalls at the lesions, and CSA and CSB proteins enhance their recognition. XPC is a damage sensor in the GGR sub-pathway of NER.

DSBs represent the most dangerous lesions that arise after IR. In eukaryotic cells, two sub-pathways of DSB repair are known: homologous recombination (HR) and nonhomologous end joining (NHEJ). Most DSBs are eliminated by NHEJ. Classical NHEJ begins with DSB end processing by the MRE11/Rad50/NBS1 (MRN) complex and end binding by Ku70/80 and DNA-PK proteins [9]. The latter phosphorylate other proteins such as RPA, WRN, and Artemis. The break is then sealed by ligase IV and its cofactors XRCC4 and XLF. The back-up sub-pathway of NHEJ involves proteins that also participate in SSB and HR repair—MRN, PARP1, and XRCC1.

HR requires the presence of a homologous sequence as a template for repair. MRN, Exo1, and other nucleases perform the 5′- to 3′-DSB end processing. The BRCA1 protein regulates MRN complex end processing after the phosphorylation and activation of ATM and checkpoint kinases. Single-stranded DNA at the 3′-ends is bound by RPA which further allows Rad52 and Rad51 protein binding. Rad51 is a central protein of HR, and it is phosphorylated by cyclin-dependent kinases which release it to bind single-stranded DNA and form nucleofilaments for homology search in sister chromatids [10,11].

Thus, the DNA repair machinery needs to be constantly active to maintain genome integrity and avoid deleterious biological consequences of DNA damage under conditions of environmental and endogenous stresses.

The detection and measurement of DNA damage is important for experimental research and is applied in clinical assays. Methods for DNA damage detection differ in their sensitivity. This chapter mainly addresses the most sensitive immunological methods that can be used for the detection of DNA damage induced by IR, UV light, and different kinds of chemical agents. Here, we present several protocols for IR damage detection that are routinely used in our laboratory.

2. THE DETECTION OF DSBs IN CULTIVATED MAMMALIAN CELLS AND TISSUES

2.1 Phosphorylated Histone H2AX as a Marker of DSBs

H2AX is known as a variant of histone H2A in mammalian cells. Its phosphorylation on Ser139 is one of the earliest events in DDR to DSBs induced by IR, nuclease action, laser irradiation, and other agents. DNA damage activates cell cycle checkpoints that stop cell cycle progression and give time for the cells to accomplish DSB repair. The members of the phosphatidylinositol 3-kinase family (PI3)—ataxia telangiectasia-mutated (ATM) and ATM-Rad3-related (ATR)—are activated

after DSB induction. ATM phosphorylates the SQ/TQ motif of its target proteins in signal transduction pathways leading to cell cycle arrest and DSB repair [12]. H2AX is phosphorylated by ATM at DSB sites in non-S-phase cells, whereas ATR phosphorylates DSBs formed at replication forks stalled at DNA lesions [13].

The phosphorylated form of H2AX (γH2AX) appears in cell nuclei within 3 min after IR and can be visualized as discrete foci using a γH2AX-specific antibody and immunofluorescence microscopy [14]. H2AX phosphorylation spreads to megabase chromatin regions surrounding DSBs. Rothkamm and Lobrich [15] have shown that the number of γH2AX foci per Gy per cell visible in the irradiated cells corresponds to the number of DSBs estimated by PFGE. Thus, the use of γH2AX as a marker of DSBs is advantageous but has some limitations. It is unknown whether γH2AX marks physical DSBs or probably registers DNA sites in which DSB ends were already sealed [16]. After completion of DSB repair, γH2AX could persist for some time at previously damaged sites, for example, due to a slow process of dephosphorylation [17].

Nevertheless, H2AX phosphorylation is successfully used for the study of spatial distribution of γH2AX foci and the estimation of kinetics of focus formation and elimination after IR exposure. The formation of γH2AX can be induced by different chemical compounds as a result of DSB induction associated with replication and repair. Monitoring γH2AX formation and cell-cycle arrest was used for the estimation of genotoxicity of different compounds used in experimental research [18]. γH2AX detection was applied for the evaluation of photogenotoxicity of chemical compounds. For that purpose, cultivated cells were treated with different environmental chemicals (benzene metabolites, photooxidized polycyclic aromatic hydrocarbons, detergents, and other substances) and exposed for 1 h to UVA at the dose correlated to the outdoor level of sunlight exposure in summer day at noon [19]. Using this approach, the risk of photocarcinogenesis after long-term exposure to low concentrations of chemicals can be predicted.

2.1.1 The Study of DSB Repair Kinetics in Cultivated Mammalian Cells

DSB repair kinetics can be studied by counting the number of γH2AX foci in individual cells after exposure to IR or other agents that induce DSBs. Bonner and colleagues [20,21] presented techniques for γH2AX detection in cultivated cells and in a variety of human and mouse tissue samples.

The maximum level of γH2AX formation was observed 1 h after IR exposure in primary human fibroblasts and Chinese hamster cells. The majority of foci were eliminated within 4–5 h after IR at the dose of 1–2 Gy [22–24]. After 7–8 h, the repair was completed, and only rare foci were seen in individual cells. These residual foci were eliminated from DNA within 1–4 days [17]. The number of spontaneous and persistent IR-induced γH2AX foci was increased in senescent cells in culture and in aging mice [25,26].

2.1.2 γH2AX Detection in Tissues of Living Organisms

The formation and elimination of DSBs after IR was studied in different mouse organs, including liver, kidney, and heart [27–30]. DSBs can be induced in noncancerous cells neighboring tumors in a so-called "bystander effect" partially associated with inflammatory cytokine production. In mice implanted with nonmetastasizing tumors, the induction of γH2AX foci was observed in distant tissues [31].

Normal and tumor tissues differ in the rate of γH2AX elimination after IR. In normal tissues, the majority of DNA damage is eliminated during 24 h post IR, while in tumors, the kinetics of γH2AX elimination is slower [32]. The analysis of DSB repair kinetics in different types of cells located in seminiferous tubules of mouse testis after total body irradiation was performed. The kinetics of DSB repair after 1 Gy irradiation was compared in undifferentiated spermatogonia, round spermatids, and somatic cells of various normal tissues. A rapid decrease of γH2AX focus number was observed in somatic tissues: only the low level of residual damage was detected 24 h post irradiation. Round spermatids and spermatogonia showed a highly increased number of γH2AX foci at 5 h post irradiation; the level of remaining foci at 24 and 48 h post irradiation was also significantly elevated indicating an impaired DSB repair capacity in these cells [33]. In mouse xenograft models of human cancer, spatiotemporal tracking of DNA damage was analyzed after intravenous injection of cell-penetrating peptide (Tat) attached covalently to ^{111}In-labeled anti-γH2AX antibody. It was found that ^{111}In-anti-γH2AX-Tat specifically targets DNA DSB and accumulates in irradiated cancer cells in vitro and in tumors in vivo following DNA damage, suggesting the potential use of radio-immunoconjugates that target γH2AX in clinical applications [34].

There are two methodological approaches for the detection of γH2AX in different mammalian tissues: immunohistochemistry and Western blotting.

There are several ways to prepare tissue sections for immunohistochemistry. Sections are prepared in the first way from paraffin-embedded formalin-fixed tissue samples and in the second way from frozen samples (eg, samples frozen in liquid nitrogen). The frozen section preparation is faster than paraffin-embedding technique and allows a good preservation of

antigens. The advantage of paraffin-embedded tissue samples is that it is easier to store them. These sections are appropriate for providing details of tissue morphology. The disadvantage of paraffin blocks is that the process of tissue preservation in formalin leads to cross-linking of certain proteins in cells. The unmasking process of cross-linked antigens (antigen retrieval) is critical for binding of the antibody to its target.

The preparation of so-called tissue touch prints is an alternative to tissue section technique. The limitations of this method are the following: first, touch prints can be prepared only from soft tissues, for example, brain and liver; and second, the method of preparation does not allow visualization of tissue morphology. However, this method is easier than the preparation of frozen or paraffin-embedded tissue sections, and we recommend it for a preliminary analysis of kinetics of γH2AX elimination in tissues.

Fluorescence microscopy is used for γH2AX detection in frozen or paraffin-embedded tissue sections. γH2AX foci can be counted in individual cells in tissue sections after using primary antibodies to γH2AX and secondary fluorescently labeled antibodies. The detection of γH2AX can be also performed with the use of the peroxidase antiperoxidase (PAP) complex antibody [35] and visualization of reaction product by light microscopy. In our research, we used primary rabbit anti-γH2AX antibodies, goat antirabbit secondary antibodies followed by the PAP complex antibody produced in rabbit which were bound by secondary antibodies. Alternatively, instead of goat antirabbit IgG of the second layer which binds to the PAP complex antibody, peroxidase-conjugated antirabbit secondary antibodies or biotin-conjugated antirabbit secondary antibodies followed by peroxidase-conjugated streptavidin can be used. This method is less advantageous than fluorescence microscopy because it does not give a possibility to count foci in individual cells but only allows estimating cells as γH2AX positive or negative (the cell is considered to be positive even if it contains a minimum number of DSBs).

It should be taken into account that some tissues contain endogenous peroxidase activity which can react with substrate solution (diaminobenzidine) and produce an undesirable background. This nonspecific background can be reduced by the pretreatment of samples with hydrogen peroxide before incubation with the PAP soluble complex antibody.

Here, we present detailed protocols for frozen tissue section and touch print preparation followed by γH2AX immunostaining used in our laboratory [28,29]. Examples of γH2AX detection in a tissue section and a touch print are presented in Fig. 37.1.

2.1.2.1 Preparation of Tissue Touch Prints

1. After ether narcosis, accurately remove an organ from the animal.
2. Slice the organ into pieces and make a flat cut through a piece of tissue with tweezers and a razor blade.
3. Place the obtained surface onto a slide with polylysine and then remove it leaving a touch print.
4. After touch printing, air dry slides for 15 min to 1 h.

2.1.2.2 Preparation of Frozen Tissue Sections

1. After ether narcosis, accurately remove an organ from the animal.
2. Using tweezers and a razor blade, take an appropriate piece of the organ.

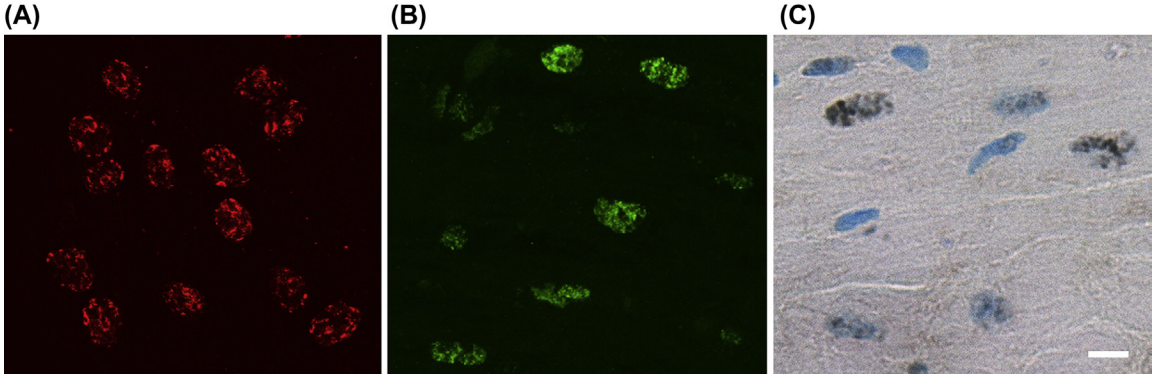

FIGURE 37.1 Immunohistochemical detection of γH2AX: (A) A touch print of Syrian hamster brain, 1 h after 5 Gy of X-ray irradiation. (B) A frozen section of Syrian hamster heart 10 μm in thickness, 1 h after 5 Gy of X-ray irradiation. Fluorescence microscopy images of cells immunostained with a mouse anti-γH2AX monoclonal antibody followed by Alexa Fluor 568 (A) and Alexa Fluor 488 (B)-conjugated secondary antibodies. (C) A frozen section of mouse heart 10 μm in thickness, 20 min after 3 Gy of X-ray irradiation. A conventional light microscopy image of cells immunostained with a peroxidase antiperoxidase soluble complex antibody (*black*). Cellular DNA was counterstained with Giemsa stain (*blue*). The majority of cells in the field of view are γH2AX-positive. The bar is 10 μm.

3. Attach the piece of the organ to a cork made from a stopper of wine bottle.
4. Immediately put the cork with the organ in liquid nitrogen.
5. Using cryostat microtome (we used Bright Co. Ltd., UK), prepare cryostat tissue sections and attach them to polylysine-treated slides.
6. Let slides to air dry for 15 min to 1 h.

2.1.2.3 Fixation and Permeabilization of Touch Prints and Tissue Sections for Fluorescence Microscopy Detection

1. Immerse slides in 2% formaldehyde (Sigma) in PBS for 20 min to fix the cells.
2. Wash slides 3 times for 5 min in PBS with gentle shaking.
3. For tissue touch prints, immerse slides in 70% ethanol chilled to −20°C for 5 min, then go to step 5.
4. For tissue sections, immerse slides in 1% Triton X-100 for 5 min; wash slides 3 times for 5 min in PBS with gentle shaking.
5. Put samples in 70% ethanol at 4°C overnight. At this step, the samples could be stored in ethanol for several days.

2.1.2.4 Fixation and Permeabilization of Tissue Sections for γH2AX Detection Using the PAP Complex Antibody

1. For fixation, immerse slides in methanol:ethanol (1:1) for 3 min.
2. Wash slides 3 times in PBS for 5 min with gentle shaking.
3. Immerse slides in 1% Triton X-100 for 5 min with gentle shaking.
4. Wash slides 2 times in PBS for 15 min with gentle shaking.

2.1.2.5 Immunohistochemical Staining of Touch Prints and Tissue Sections for Fluorescence Microscopy γH2AX Detection

1. Wash slides after ethanol storage (see Section 2.1.2.3) 2 times in PBS for 5 min with gentle shaking.
2. Block nonspecific antibody binding by incubation in PBS supplemented with 8% bovine serum albumin (BSA) at 37°C for 30 min. BSA should be prepared freshly before the experiment.
3. Wash slides in PBS for 5 min.
4. Incubate slides with primary rabbit polyclonal antibodies to γH2AX (1:200, Abcam) in 1% BSA-PBS at 37°C for 1 h. For frozen sections, sometimes it is better to incubate slides overnight at 4°C.
5. Wash slides 3 times in PBS for 5 min with gentle shaking.
6. Incubate slides with Alexa 488 (568)- or FITC-conjugated goat antirabbit antibodies (1:200, Invitrogen) at 37°C for 40 min.
7. Wash slides 3 times in PBS for 5 min with gentle shaking.
8. For nuclear staining, incubate slides with 4′,6-diamidino-2-phenylindole (DAPI) (0.05 μg/mL) in PBS in the darkness for 10 min.
9. Wash slides in PBS for 5 min with gentle shaking.
10. Mount slides in antifade solution. We used Citifluor glycerol/PBS antifade solution (Marivac, Canada).
11. Store slides in a box at 4°C.

2.1.2.6 Immunohistochemical Staining of Tissue Sections for Light Microscopy γH2AX Detection

1. Block endogenous peroxidase activity by immersing slides in 70% methanol containing 0.3% H_2O_2 at room temperature for 30 min.
2. Wash slides 3 times in PBS for 5 min with gentle shaking.
3. Block nonspecific antibody binding by incubation in PBS + 0.1% Tween 20 (PBST) supplemented with 5% bovine serum albumin (BSA-PBST) at room temperature for 30 min.
4. Wash slides 3 times in PBS for 5 min with gentle shaking.
5. Incubate slides with primary rabbit polyclonal antibodies to γH2AX (1:200, Abcam) in 1% BSA-PBST at 4°C overnight.
6. Wash slides 3 times in PBST for 10 min with gentle shaking.
7. Incubate slides with secondary goat antirabbit antibodies in 1% BSA-PBST for 1 h at room temperature.

8. Wash slides 3 times in PBST for 10 min with gentle shaking.
9. Incubate slides in PAP soluble complex antibody produced in rabbit (1:100, Sigma) in 1% BSA-PBST at 4°C overnight.
10. Wash slides 3 times in PBST for 10 min with gentle shaking.
11. Wash slides in PBS for 5 min with gentle shaking.
12. Apply diaminobenzidine (10 mg diaminobenzidine dissolve in 10 mL of PBS and mix with 0.03–0.1% solution of H_2O_2 in PBS) for 5–10 min.
13. Wash slides in running tap water. If the reaction is weak, sections could be further incubated with diaminobenzidine cobalt acetate for 5 min and then washed in running tap water.
14. Stain nuclei with Giemsa stain.
15. Dehydrate slides in the increasing ethanol concentrations (70%, 80%, 96%) for 2–5 min in each.
16. Incubate slides in xylen 3 times for 5 min at room temperature.
17. Embed slides in Canada balsam.

2.1.2.7 Western Blotting of γH2AX in Animal Tissues

Western blotting technique is often used to study the relative efficiency of γH2AX formation in different tissues. To prepare samples for electrophoresis, tissues need to be lysed in order to release the protein of interest. For the detection of nuclear proteins by conventional protocols, it is recommended to use RIPA buffer (radio-immunoprecipitation assay buffer). During lysis, proteolysis may occur which can be slowed down by keeping samples on ice and using appropriate cocktails of inhibitors. The preparation of lysate from a tissue with RIPA buffer takes about 3 h.

Here, we present an easier and faster protocol for the preparation of lysates from tissues with 4x Laemmli buffer without adding proteolysis inhibitors. The main disadvantage of this method is that protein concentration cannot be measured in the samples. However, in our hands, this method works accurate when we weigh tissue samples carefully and add the corresponding volume of buffer. The total protein concentration in the samples can be controlled using antibodies to housekeeping proteins (for example, beta-actin). The densitometry of housekeeping protein bands can be used for the comparison of protein concentrations in different samples.

The steps of the protocol are the following:

1. After ether narcosis, accurately remove an organ from the animal.
2. Using tweezers and a razor blade, take an appropriate piece of the organ.
3. Put the piece of the organ in an eppendorf tube and put it in liquid nitrogen immediately.
4. Using a ceramic mortar and liquid nitrogen, homogenize the piece of the organ to a state of powder.
5. Weigh the powder in an eppendorf tube (an empty tube should be previously weighted) and add 300 μL of 4x SDS-gel-loading buffer with b-MetOH (200 mM Tris–HCl (pH 6.8), 4% SDS, 400 mM b-MetOH, 40% Glycerol, 0.01% Bromphenol blue) to 5 mg of the tissue.
6. Mix well by vortexing and incubate 10 min at 95°C with shaking.
7. Mix well by vortexing and centrifuge at 12,000 rpm for 10 min at 4°C.
8. Take the supernatant and aliquot it into the samples.
9. Store the samples at −70°C. Alternatively, the samples could be stored at −20°C. The samples could be used for gel electrophoresis immediately; however, we recommend to freeze them first.
10. On the day of electrophoresis, take the samples from the freezer and heat them for 2 min at 95°C.
11. Load the samples on a gel along with a molecular weight marker. We recommend to use 15% SDS-PAGE for γH2AX.
12. First, run the gel at 60 V for about 15 min, and then at 120 V.
13. Transfer proteins from the gel to a Hybond-C nitrocellulose membrane (Amersham) by electroblotting for 1 h at 100 V. We recommend to use the Towbin buffer for the transfer (25 mM Tris, 192 mM glycine, 20% (v/v) methanol).
14. Block the membranes in 5% nonfat dry milk in PBS containing 0.1% Tween 20 at 4°C overnight. By our experience, overnight blocking gives the best results.
15. Wash the membranes 2 times in PBST for 10 min with shaking.
16. Incubate the membranes in the primary mouse monoclonal antibody to γH2AX (1:2000, Abcam) for 2 h at room temperature with gentle shaking.
17. Wash the membranes 3 times in PBST for 10 min with shaking.
18. Incubate the membranes with horseradish peroxidase-labeled goat antimouse IgG (1:15,000, Zymax) for 1 h at the room temperature with gentle shaking.
19. Visualize immunoblots with Immobilon Western Chemiluminescent HRP Substrate (Millipore).

2.2 Imaging of DSB Repair Proteins at Chromatin Sites Marked by γH2AX in Cultivated Mammalian Cells

H2AX located at chromatin domains surrounding DSBs is phosphorylated by ATM and DNA-PK. ATM is recruited and activated by the MRN protein complex [36]. When inactive, ATM exists in a dimeric form. In IR-damaged cells, the subunits of the dimer dissociate and become active after phosphorylation [37]. ATM is considered to be a major kinase involved in H2AX phosphorylation after DSB induction [38,39]. It plays a predominant role in γH2AX phosphorylation after IR, but in the case of ATM deficiency, it can be substituted by DNA-PK. It has been shown that H2AX phosphorylation kinetics are normal in $ATM^{-/-}$ and $DNA\text{-}PK^{-/-}$ cells [40,41]. However, the conclusion that ATM and DNA-PK can redundantly substitute each other is not supported by some research groups (reviewed in Ref. [28]).

At the sites of DSBs, γH2AX attracts a number of repair proteins which can be visualized using the corresponding antibodies. Fig. 37.2 represents an example of double immunostaining of γH2AX and 53BP1 or phospho-(Ser 2056)-DNA-PK proteins in G0 Syrian hamster fibroblasts after bleomycin treatment.

Intriguingly, all the proteins we have analyzed (53BP1, phospho-(Ser 2056)-DNA-PK, and phospho-(Ser 1981)-ATM) colocalize with γH2AX at the sites of DSBs. 53BP1 and ATM represent the proteins involved in HR, and DNA-PK is a central protein of NHEJ. It has been reported by P. Jeggo and collaborators that ATM is involved in the repair of approximately 15% of IR-induced DSBs, and 85% of DSBs are repaired in an ATM-independent manner. Moreover, these 15% of DSBs are located at the periphery of the nucleus in the area occupied by heterochromatin [42]. In contrast, we observed a uniform distribution of γH2AX colocalized with phospho-ATM within the nuclei of mammalian cells. It was proposed earlier that proteins involved in NHEJ and HR compete for DSBs [9]. Our observation that proteins of both sub-pathways accumulate at chromatin sites marked by γH2AX supports this suggestion.

In the analysis of protein colocalization in individual cells, the determination of the stage of cell cycle is sometimes necessary. For that purpose, we used staining with antibody to Ki-67, a marker of proliferation, and a nucleoside analog 5-ethynyl-2′-deoxyuridine (EdU) incorporation for the labeling of S-phase cells. Ki-67 nuclear distribution is cell-cycle dependent, and its patterns have been described for normal human fibroblasts and embryonic stem cells [43,44]. G0 cells are Ki-67-negative, and proliferative cells are Ki-67-positive. We recommend using fluorescently labeled EdU for the determination of S-phase cells. Ki-67 staining patterns in G2 cells are easily recognized; these cells contain one or two round-shaped and brightly stained nucleoli on a faint background. Thus, as a result of this approach, G0 cells are $Ki\text{-}67^{-}/EdU^{-}$, G1 cells are $Ki\text{-}67^{+}/EdU^{-}$, S-phase cells are $Ki\text{-}67^{+}/EdU^{+}$, and G2 cells $Ki\text{-}67^{+}/EdU^{-}$ (but well distinguished from G1 due to a different distribution of Ki-67). Here, we present protocols for γH2AX/DSB repair protein/Ki-67 immunostaining of cells after incorporation of EdU which is fluorescently labeled

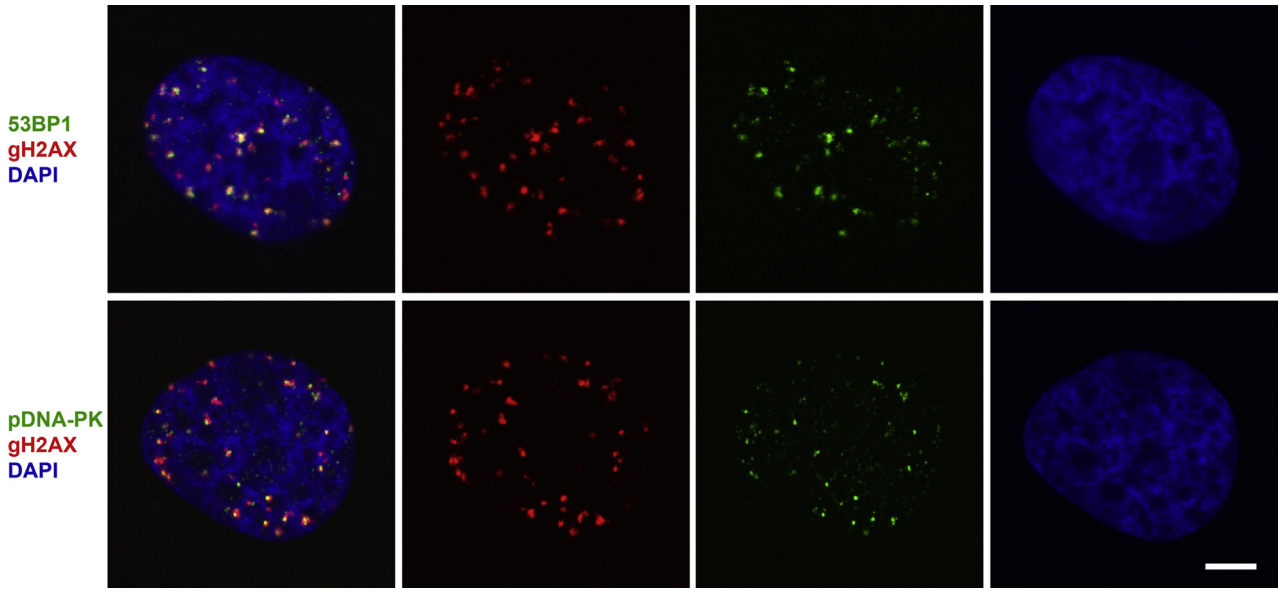

FIGURE 37.2 The visualization of DSBs by double-immunostaining of γH2AX and pDNA-PK or 53BP1 repair proteins in Syrian hamster fibroblasts. DNA in the nuclei is counterstained with DAPI. The bar is 5 μm.

by Click-iT technology with Alexa Fluor dye in a specific reaction developed by ThermoFisher Scientific (Click-iT EdU Alexa Fluor 647 Imaging Kit).

2.2.1 *Immunofluorescence Microscopy Protocol for a Simultaneous Visualization of γH2AX and pDNA-PK/pATM/53BP1 Repair Proteins in Asynchronously Growing Cells That Allows to Discriminate S-phase Cells*

2.2.1.1 Sample Preparation and Fixation

1. The day before experiment, plate $0.3–0.5 \times 10^5$ cells on cover-glass slides 24 mm × 24 mm in Petri dishes with a 35 mm diameter (the density of plating depends on the cell line used). For growing mammalian fibroblasts, we use Minimal essential medium supplemented with 10–12% fetal bovine serum, 100 U/mL penicillin-streptomycin mixture, and 4 mM L-glutamine. Grow the cells overnight in a CO_2 incubator under conventional conditions of cultivation at 5% CO_2.
2. Treat the cells with IR, bleomycin, or other agent of interest. Keep the cells in a CO_2 incubator for the appropriate time after the treatment. 10–30 min before fixation, add EdU to the growth medium in the optimal concentration for your cell type (10 μM final concentration is recommended by the manufacturer as the optimized concentration for A549, HeLa, and NIH/3T3 cells) (ThermoFisher Scientific, Click-iT EdU Alexa Fluor 647 Imaging Kit).
3. Rinse coverslips twice with PBS and fix with 3.7% formaldehyde in PBS for 15 min at the room temperature. Rinse the cells twice with 3% BSA solution in PBS, permeabilize with 0.5% Triton X-100 in PBS for 20 min at the room temperature, then wash the cells twice with 3% BSA in PBS.

2.2.1.2 Click-iT Technology: Fluorescent Labeling of EdU

Treat the cells on coverslips in the darkness with reagents of Click-iT reaction cocktail including Alexa Fluor 647 azide, triethylammonium salt for 30 min.

For example, for two coverslips, prepare the following mixture of components from the Kit: 86 μL 1x Click-iT reaction buffer working solution; 4 μL $CuSO_4$ solution (100 mM); 0.24 μL Alexa Fluor 647 azide working solution; 10 μL Reaction buffer additive prepared fresh by diluting 10x stock solution in deionized water.

Use 50 μL of this reaction cocktail for each coverslip within 15 min of preparation. We recommend to place the coverslips with the cells on a piece of Parafilm (Sigma) on the bottom of a Petri dish. Lay each coverslip (the surface covered with cells) on a drop of reaction cocktail. After incubation, wash the cells on coverslips twice with 3% BSA in PBS, then proceed to nuclear protein and DNA staining.

2.2.1.3 Immunostaining Procedure

1. Rinse the cells on coverslips in PBS and incubate in 1% Blocking Reagent (Roche, Cat N. 1,096,176) in PBS with 0.02% Tween 20 for 30 min.
2. Dilute all antibodies to final concentrations recommended by the manufacturer in 0.5% Blocking Reagent (Roche) solution with 0.02% Tween 20.
3. Incubate the cells on the coverslips with the mixture of the primary antibodies at 37°C for 1 h. We recommend to place coverslips in a humid chamber on a piece of Parafilm on a drop of antibodies diluted in Step 2 (40–50 μL for each coverslip 24 mm × 24 mm).

The mixture of the primary antibodies is one of the following:

Either: rabbit polyclonal anti-gH2AX (Abcam, 1:100) and mouse monoclonal antiphospho-ATM (S1981) (Abcam, 1:100), or mouse monoclonal anti-γH2AX (Millipore (Upstate), 1:200) and rabbit polyclonal anti-53BP1 (1:200), or mouse monoclonal anti-γH2AX (Millipore (Upstate), 1:200) and rabbit polyclonal antiphospho-DNA-PK (S2056) (Abcam, 1:100).

4. Wash the slides twice (for 30 min in total) after incubation by shaking in PBS supplemented with 0.1% Tween 20.
5. Incubate the cells on the coverslips with the mixture of secondary antibodies: Alexa Fluor 568-conjugated polyclonal goat antirabbit IgG (Invitrogen, 1:400) and Alexa Fluor 488-conjugated polyclonal goat antimouse (Invitrogen, 1:400) at 37°C for 40 min.
6. Wash the coverslips for 30 min as described in Step 4.
7. Counterstain the DNA with 0.5 μg/mL DAPI in PBS and mount in an antifade solution. We used Citifluor antifade solution (Marivac, Canada).

2.2.2 Immunofluorescent Detection of γH2AX in Different Phases of Cell Cycle as Determined Using Ki-67 Staining and EdU Incorporation

This protocol is mostly similar to the protocol described in Section 2.2.1. The difference is in the description of double-immunostaining procedure. Here, in Section 2.2.1.3 (Step 3), the content of the mixture of primary antibodies should be the following:

Mouse monoclonal anti-γH2AX (Millipore (Upstate), 1:200) and rabbit polyclonal anti-Ki-67 (Abcam, 1:200).

2.2.3 Immunofluorescence Microscopy Protocol for a Simultaneous Visualization of γH2AX and pDNA-PK/pATM/53BP1 Repair Proteins in Asynchronously Growing Cells That Allows Discriminating Cells in G0, G1, S, and G2 Phases of Cell Cycle

We suggest this protocol for double γH2AX/Ki-67 immunostaining of cells transiently transfected with a GFP-fused repair protein (pDNA-PK, pATM or 53BP1) after EdU incorporation in DNA.

In the majority of steps, this protocol is similar to the protocol described in Section 2.2.1. The difference is that the cells should be transiently transfected with a GFP-conjugated protein of your choice. Follow the protocol (Section 2.2.1) up to the description of immunostaining procedure (Section 2.2.1.3). Here, this step should be the following:

1. This step is the same as in Section 2.2.1.3.
2. This step is the same as in Section 2.2.1.3.
3. Follow Step 3 as described in Section 2.2.1.3 up to the preparation of the mixture of primary antibodies. Here, the mixture of primary antibodies should be the following:
   Mouse monoclonal anti-γH2AX (Millipore, 1:200) and rabbit polyclonal anti-Ki-67 (Abcam, 1:200).
4. This step is the same as in Section 2.2.1.3.
5. Incubate the cells on the coverslips at 37°C for 40 min with the mixture of secondary antibodies: Alexa Fluor 568-conjugated polyclonal goat antimouse IgG (Invitrogen, 1:400) and Alexa Fluor 405-conjugated polyclonal goat antirabbit (ThermoFisher Scientific, Cat No. A-31,556, dilute according to the manufacturer's recommendations).
6. Wash the coverslips for 30 min as described in Step 4.
7. Mount the cells on the slides in an antifade solution. We used Citifluor antifade solution (Marivac, Canada).

2.2.4 Microscopy and Image Acquisition

For image acquisition, the confocal Leica TCS SP5 system equipped with HCX PL APO 100x/1.4 and 40x/1.25 oil immersion objectives, 488 nm argon, 543 nm HeNe, 633 nm HeNe and 405 nm diode lasers and Leica LAS AF software were used.

Red (Alexa Fluor 568), far-red (Alexa Fluor 647), green (Alexa Fluor 488), and blue (DAPI) fluorescence were acquired sequentially to avoid fluorophore emission bleed-through artifacts.

3. γH2AX IN BIODOSIMETRY AND CLINICAL ASSAYS

Historically, the biodosimetry method was represented by cytogenetic dosimetry based on chromosome aberration analysis that offered a reliable means for estimating biological exposure to radiation. The γH2AX assay is a new and powerful tool in biodosimetry. The linear radiation dose-response relationship has been shown in experimental and clinical studies using γH2AX as a biomarker for ionizing radiation exposure. For this kind of analysis, peripheral blood lymphocytes of patients are the most easily obtainable cells. Even after low-dose radiation exposure, the measurement of γH2AX focus number is reliable [20]. Scoring of dicentric chromosomes and analysis of γH2AX focus formation in lymphocytes of healthy donors after computer tomography scans (at dose levels from 0.025 to 1 Gy) demonstrated that both methods are equally sensitive when estimating radiation-induced damage after low-dose IR [45]. γH2AX focus counting was successfully used for the estimation of radiation risks in pediatric patients with congenital heart disease who underwent cardiac catheterization procedures and received radiation doses less than 50 mSv [46]. Flow cytometry was also used to measure H2AX phosphorylation, and it was shown to be a reliable and more rapid approach than γH2AX focus scoring in individual cells [47].

γH2AX assays are helpful for monitoring a patient's progress during the treatment of cancer. The detection of γH2AX foci in lymphocytes can be used for the identification of patients with an increased radiosensitivity who have the highest risk of radiotherapy-related side effects [48]. A promising assay for monitoring the effect of anticancer therapy was based on the measurement of γH2AX in tumor cells dissociated from tumors and circulating in the blood [49]. Many other examples of using γH2AX in cancer research and clinical trials are provided in the review of Ivashkevich and colleagues [50].

4. COMET FLUORESCENCE IN SITU HYBRIDIZATION (COMET-FISH) IN THE DETECTION OF DIFFERENT TYPES OF DNA DAMAGE

The Comet assay is valuable for the elucidation of genotoxicity and DNA repair. It is widely used for the detection of IR lesions, including SSBs and DSBs. Enzyme-modified assays utilizing DNA damage-specific endonucleases such as thymine glycol DNA glycosylase–Endo III and formamidopyrimidine DNA glycosylase (FPG) were proposed for the detection of oxidized DNA lesions using the Comet technique (reviewed in Refs. [51,52]).

A simultaneous visualization of DSBs and SSBs can be performed in a two-tailed Comet assay (TT-comet) using two-dimensional electrophoresis. This modified Comet assay was used, for example, in the analysis of mammalian sperm for the evaluation of the influence of SSBs and DSBs on male infertility [53].

Comet-FISH can be applied to DNA damages induced by IR, different chemical agents, and products of cellular metabolism that can be converted to SSBs or DSBs [54]. It allows the possibility to compare the level of DNA damage and the effectiveness of its repair in certain regions of the genome. Comet-FISH is a combination of two well-known methods: the Comet assay (single-cell gel electrophoresis) and fluorescence hybridization in situ. It is a sensitive and rapid method for the detection of DNA damage. A detailed description of this technique was presented in Methods in Molecular Biology by different authors [54–56].

Briefly, cells placed in low-melting agarose on the surface of microscope slides are subjected to electrophoresis after the action of a damaging agent. In alkaline single-cell electrophoresis, comet tails are formed by DNA loops migrated from cells in the electric field. The size of a comet tail in an individual cell is proportional to the level of DNA damage. The number of fluorescent signals in comet tails gives information about the damage in the gene of interest and its repair.

Using Comet-FISH, the rate of IR-induced DSB repair was compared in TP53 and hTERT genes [57]. The TP53 gene was repaired more rapidly in normal cells than in cells of Cockayne syndrome cell line that was defective in transcription-coupled repair.

Using Comet-FISH technique with labeled single-stranded probes and a specific endonuclease, the transcription-coupled repair of CPDs in the ATM gene was documented in human fibroblasts irradiated at a low UV dose (0.1 J/m^2). 8-oxoG was also preferentially repaired in the transcribed strand of the ATM gene which was revealed using a specific glycosylase in the Comet-FISH assay [58].

The TP53 fragmentation rate was estimated by the alkaline Comet assay and Comet-FISH in lymphocytes of pharmaceutical industry workers after a prolonged exposure to phenylhydrazine, ethylene oxide, dichloromethane, and 1,2-dichloroethane. It was shown that exposure to carcinogens affected the structural integrity of TP53, and the use of personal protective equipment decreased the risk of exposure [59].

Comet-FISH has a potential to be used in understanding the impact of genotoxicity on animal physiology. The effect of hydrogen peroxide on nuclear organizer regions in Pacific oyster *Crassostea gigas* was analyzed by this technique [60].

5. METHODS FOR STUDYING DNA REPAIR AFTER UV

Two different strategies have been used for the detection of UV-induced DNA lesions. Direct methods are based on analytical chemistry requiring first the extraction and then the digestion of DNA followed by the measurement of specific DNA lesions using a specific detector coupled to chromatographic separation. Indirect biochemical methods based on the quantitation of DNA strand breaks produced by UV-lesion repair enzymes have been also developed. Detection methods based on the use of specific antibodies raised against UV lesions and UV-damage repair proteins are mostly used at the present time.

In 1991, Mori and coauthors successfully established new monoclonal antibodies (IgG class) specific to UV-induced DNA damages: CPDs and (6-4)PPs [61]. It was the first report of the simultaneous establishment of monoclonal antibodies raised for different types of UV-induced DNA damages. Antibodies specific for CPDs and (6-4)PPs have been largely used in immunological approaches (ELISA, slot blot technique, fluorescence microscopy), for in vitro and in vivo detection of UV lesions, and for studies of their repair efficiency [62,63]. These approaches offer a number of advantages, including the ability to perform analysis of a large number of samples in ELISA, and the need of a small number of cells for the quantification of immunostained cells under a fluorescent microscope. However, they are limited in sensitivity and cannot detect a relatively small number of repair events which occur within minutes after UV irradiation. A very sensitive non-radioisotopic method for the detection of oligonucleotides excised during NER was developed in 2014 [64]. The excised oligonucleotides isolated from cells were labeled with biotin, separated by gel electrophoresis, transferred to a nylon membrane, and incubated with HRP-conjugated streptavidin for chemiluminescence detection after the immobilization. Using this method, the repair of UV lesions can be detected within 6 min after UV irradiation at the dose of 10 J/m^2.

Both TCR and GGR result in the excision of about 30-base oligonucleotides containing the DNA lesion [65] followed by DNA repair synthesis (DRS) to fill the resulting gap with undamaged nucleotides and ligation [66–68]. Immunofluorescent detection of incorporated halogenated deoxyuridines, 5-iododeoxyuridine (IdU), and 5-chlorodeoxyuridine (CldU), has been used for the analysis of UV-induced DRS in mammalian cells [69,70]. It has been found that when both precursors are added simultaneously to UV-irradiated non-S-phase human fibroblasts and incubated for 2 h, they label different sites in the nucleus that might be due to the compartmentalization of I-dUTP and Cl-dUTP pools. In contrast, even very short periods of IdU plus CldU labeling of S-phase cells produced IdU and CldU replication foci that were mostly overlapped [70].

The DRS-dependent incorporation of IdU is very low, but a fluorescent signal can be amplified using the tyramide signal amplification (TSA) system allowing a reliable detection of DRS foci in human cells at a very short duration (10 min) of IdU labeling after UV irradiation [69]. The TSA system is an enzyme-mediated detection method that uses horseradish peroxidase (HRP) to generate a high-density labeling of a target protein or nucleic acid in situ. Taking into account that each individual repair synthesis patch is about 30-base long which is not sufficient for DRS detection using indirect immunofluorescence even with the TSA system, it is likely that the detected discrete foci of DRS represent clusters of several DRS patches [69].

In the 1980s, it was found that the proliferating cell nuclear antigen (PCNA) changes its solubility in methanol after its recruitment to DNA in undamaged S-phase cells [71] and becomes insoluble in methanol in G1/G2 cells only after UV irradiation [72], suggesting that its insolubilization may be associated with the involvement of PCNA in DNA resynthesis step of NER. The UV-induced insolubilization after Triton X-100 treatment was observed for XPA and XPB NER proteins [73]. Using a local UV-irradiation technique, a sequential immobilization of NER factors was demonstrated in irradiated spots [74,75].

H2AX phosphorylation in response to IR and chemical drugs attracts the major attention of scientists, but its role in UV-damage response is not completely characterized. It was shown by Halicka et al. that according to data obtained by flow cytometry, the highest degree of H2AX phosphorylation induced by UV occurred in S-phase cells; in G1, G2, and M cells, the degree of H2AX phosphorylation was markedly lower than that in S-phase cells, and it was strongly UV dose-dependent [76]. We demonstrate in Fig. 37.3 that CPD-positive regions colocalize almost completely with γH2AX staining after UV irradiation using polycarbonate filters with pores [77].

Immunofluorescent analysis revealed that H2AX was phosphorylated by ATR kinase at replication forks blocked by UV lesions in S-phase cells [78]. In contrast, UV-induced H2AX phosphorylation in non-S-phase cells did not occur due to DNA DSB formation, but was rather triggered by DNA repair intermediates [79,80].

It was demonstrated that ATR kinase participated in UVC induction of H2AX phosphorylation in nonreplicating cells [80]. Other researchers reported that high doses of UVA irradiation strongly induced H2AX phosphorylation in nuclei that was mediated by c-Jun N-terminal kinase (JNK), and the phosphorylation of H2AX by JNK was associated with the induction of apoptosis [81]. Thus, in non-S-phase cells, H2AX phosphorylation is NER-dependent and associated with ATR, while JNK contributes to H2AX phosphorylation after the induction of apoptosis.

Besides these approaches, a recently suggested method for monitoring the repair of UV-induced (6-4)PPs with a purified DNA damage-binding protein 2 complex (DDB2) should be mentioned. The recognition of UV-damaged DNA by

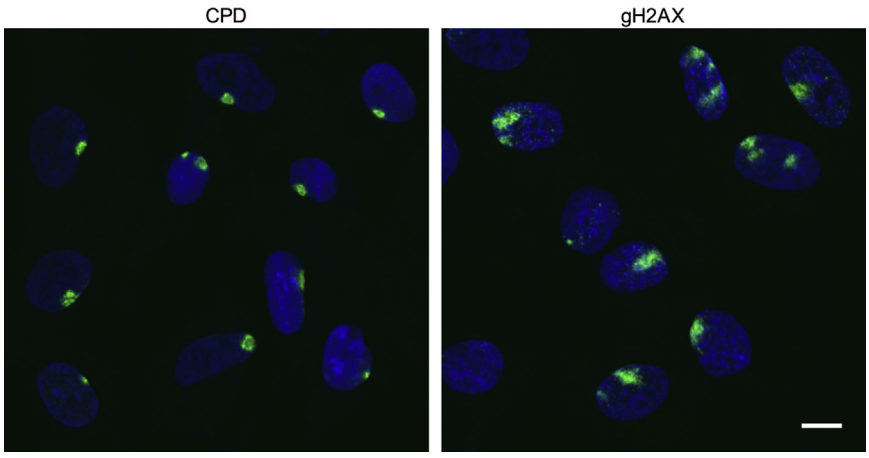

FIGURE 37.3 The visualization of UV damages after local irradiation of Syrian hamster fibroblasts. Irradiation at the dose of 100 J/m^2 was performed using isopore filters with a pore diameter 5 μm placed over the cell monolayer. Fluorescence microscopy images of fibroblasts immunostained with mouse anti-CPD antibody and mouse anti-γH2AX antibody followed by Alexa Fluor 488-conjugated secondary antibodies. The bar is 10 μm.

DDB2 is necessary for the recognition of UV lesions in GGR [82]. DDB2 binds both types of UV lesions, but it has a higher affinity for (6-4)PPs compared to CPDs [83]. FLAG-HA-tagged DDB2 protein (DDB2 proteo-probe) stably expressed in HeLa S3 cells was purified using affinity chromatography and added to cells irradiated by different sources of UV (UVA, UVB, UVC). DDB2 proteo-probe-binded (6-4)PPs that were induced preferentially by UVB and UVC but not by UVA suggest a possible use of this probe for the recognition and monitoring the repair of this certain type of UV lesions [84].

6. CONCLUSIONS

The maintenance of genome stability is important for all living organisms. In this chapter, some examples of DNA damage detection technologies are presented. A particular attention is paid to immunological methods that are commonly used for the detection and quantification of DNA damage. These methods are useful for detecting damages induced by IR, UV, and chemical carcinogens.

Here, we mainly describe γH2AX-based methods for the detection of IR-induced DNA damage and repair. The immunofluorescence microscopy technique allows the visualization and scoring of γH2AX foci and foci of different repair proteins in individual cells, and it is also useful for analysis of DSB repair. We provide several protocols for γH2AX detection in cultivated mammalian cells and tissues which might be useful for readers. The protocols for cultivated mammalian cells include the fixation and double-immunostaining of γH2AX in combination with some DSB repair proteins. The procedure of immunostaining allows the possibility to discriminate cells in different phases of cell cycle. We provide a tissue-processing technique for sectioning and γH2AX immunostaining as well as a detailed description of tissue sample preparation for electrophoresis and immunoblotting which includes some innovations in comparison with the conventionally used techniques.

The indirect approach of DSB detection utilizing γH2AX assays is important not only in basic research but also in clinical practice. Anticancer therapeutic strategies are mainly based on introducing DSBs in cancer cells. While some anticancer compounds induce DSBs directly, others produce non-DSB types of lesions that can lead to DSB formation during the process of DNA repair. The measurement of cellular γH2AX levels can be used for the estimation of chemotherapy effectiveness and radiosensitivity of patients and for the prediction of anticancer treatment toxicity. It is reasonable to expect that the importance of γH2AX assays will continue to increase in the future, and γH2AX techniques will be improved, thus giving an opportunity to broaden the scope of their applications in clinical trials.

GLOSSARY

DDB2 proteo-probe Represents the UV-induced DNA damage recognition protein DDB2 fused with FLAG-HA tag. The probe recognizes the UV-irradiated DNA in a number of assays, including cytochemistry, histochemistry, flow cytometry, slot-blotting, and DNA pull-down assays [84].

LIST OF ABBREVIATIONS

6-4PP Pyrimidine (6-4) pyrimidone photoproducts
8-oxo-guanine 7,8-Dihydro-8-oxogunine
AP sites Apurinic/apyrimidinic (abasic) sites
ATM Ataxia telangiectasia mutated
ATR ATM-Rad3 related
BER Base excision repair
BSA-PBST PBST supplemented with 5% bovine serum albumin
CldU 5-Chlorodeoxyuridine
Comet-FISH Comet fluorescence in situ hybridization
CPD Cyclobutane pyrimidine dimer
DAPI 4′,6-Diamidino-2-phenylindole
DDB2 DNA damage-binding protein 2 complex
DDR Cellular DNA damage response
DSBs Double-strand DNA breaks
EdU 5-Ethynyl-2′-deoxyuridine
GGR Global genomic repair
HR Homologous recombination
IdU 5-Iododeoxyuridine
IR Ionizing radiation

JNK c-Jun N-terminal kinase
MRN MRE11/Rad50/NBS1 complex
NER Nucleotide excision repair
NHEJ Nonhomologous end joining
PAP Peroxidase antiperoxidase
PBST PBS+0.1% Tween 20
PI3 Phosphatidylinositol 3-kinase family
ROS Reactive oxygen species
SSBs Single-strand DNA breaks
TCR Transcription-coupled repair
TSA Tyramide signal amplification
γH2AX Phosphorylated form of H2AX

ACKNOWLEDGMENTS

We are grateful to Dasha Zaytseva for careful proofreading of the manuscript. This work was supported by the grant from the Russian Foundation for Basic Research 13-04-00442a.

REFERENCES

[1] Dizdaroglu M. Oxidative damage to DNA in mammalian chromatin. Mutat Res 1992;275(3–6):331–42.
[2] Cooke MS, et al. Oxidative DNA damage: mechanisms, mutation, and disease. FASEB J 2003;17(10):1195–214.
[3] Sinha RP, et al. UV-induced DNA damage and repair: a review. Photochem Photobiol Sci 2002;1(4):225–36.
[4] Rastogi RP, et al. Molecular mechanisms of ultraviolet radiation-induced DNA damage and repair. J Nucleic Acids 2010;2010:592980.
[5] Muller PA, et al. Mutant p53 in cancer: new functions and therapeutic opportunities. Cancer Cell 2014;25(3):304–17.
[6] Kim Y-J, et al. Overview of base excision repair biochemistry. Curr Mol Pharmacol 2012;5(1):3–13.
[7] Hanawalt PC. Subpathways of nucleotide excision repair and their regulation. Oncogene 2002;21(58):8949–56.
[8] Spivak G, et al. The complex choreography of transcription-coupled repair. DNA Repair (Amst) 2014;19:64–70.
[9] Shrivastav M, et al. Regulation of DNA double-strand break repair pathway choice. Cell Res 2008;18(1):134–47.
[10] Polo SE, et al. Dynamics of DNA damage response proteins at DNA breaks: a focus on protein modifications. Genes Dev 2011;25(5):409–33.
[11] Summers KC, et al. Phosphorylation: the molecular switch of double-strand break repair. Int J Proteomics 2011;2011:373816.
[12] Osborn AJ, et al. Checking on the fork: the DNA-replication stress-response pathway. Trends Cell Biol 2002;12(11):509–16.
[13] Zou L, et al. Sensing DNA damage through ATRIP recognition of RPA-ssDNA complexes. Science 2003;300(5625):1542–8.
[14] Rogakou EP, et al. DNA double-stranded breaks induce histone H2AX phosphorylation on serine 139. J Biol Chem 1998;273(10):5858–68.
[15] Rothkamm K, et al. Evidence for a lack of DNA double-strand break repair in human cells exposed to very low x-ray doses. Proc Natl Acad Sci USA 2003;100(9):5057–62.
[16] Kinner A, et al. Gamma-H2AX in recognition and signaling of DNA double-strand breaks in the context of chromatin. Nucleic Acids Res 2008;36(17):5678–94.
[17] Löbrich M, et al. gammaH2AX foci analysis for monitoring DNA double-strand break repair: strengths, limitations and optimization. Cell Cycle 2010;9(4):662–9.
[18] Ando M, et al. Usefulness of monitoring γ-H2AX and cell cycle arrest in HepG2 cells for estimating genotoxicity using a high-content analysis system. J Biomol Screen 2014;19(9):1246–54.
[19] Ibuki Y, et al. Evaluation of chemical phototoxicity, focusing on phosphorylated histone H2AX. J Radiat Res 2015;56(2):220–8.
[20] Redon CE, et al. γ-H2AX detection in peripheral blood lymphocytes, splenocytes, bone marrow, xenografts, and skin. Methods Mol Biol 2011;682:249–70.
[21] Nakamura A, et al. Techniques for gamma-H2AX detection. Methods Enzymol 2006;409:236–50.
[22] Nazarov IB, et al. Dephosphorylation of histone gamma-H2AX during repair of DNA double-strand breaks in mammalian cells and its inhibition by calyculin A. Radiat Res 2003;160(3):309–17.
[23] Svetlova M, et al. Elimination of radiation-induced gamma-H2AX foci in mammalian nucleus can occur by histone exchange. Biochem Biophys Res Commun 2007;358(2):650–4.
[24] Solovjeva LV, et al. Forskolin decreases phosphorylation of histone H2AX in human cells induced by ionizing radiation. Radiat Res 2009;171(4):419–24.
[25] Endt H, et al. Detailed analysis of DNA repair and senescence marker kinetics over the life span of a human fibroblast cell line. J Gerontol A Biol Sci Med Sci 2011;66(4):367–75.
[26] Sedelnikova OA, et al. Delayed kinetics of DNA double-strand break processing in normal and pathological aging. Aging Cell 2008;7(1):89–100.
[27] Koike M, et al. Tissue-specific DNA-PK-dependent H2AX phosphorylation and gamma-H2AX elimination after X-irradiation in vivo. Biochem Biophys Res Commun 2008;376(1):52–5.
[28] Firsanov DV, et al. H2AX phosphorylation at the sites of DNA double-strand breaks in cultivated mammalian cells and tissues. Clin Epigenetics 2011;2(2):283–97.

[29] Firsanov D, et al. Dynamics of γH2AX formation and elimination in mammalian cells after X-irradiation. Biochimie 2012;94(11):2416–22.
[30] Gavrilov B, et al. Slow elimination of phosphorylated histone gamma-H2AX from DNA of terminally differentiated mouse heart cells in situ. Biochem Biophys Res Commun 2006;347(4):1048–52.
[31] Redon CE, et al. Tumors induce complex DNA damage in distant proliferative tissues in vivo. Proc Natl Acad Sci USA 2010;107(42):17992–7.
[32] Bañuelos CA, et al. gammaH2AX expression in tumors exposed to cisplatin and fractionated irradiation. Clin Cancer Res 2009;15(10):3344–53.
[33] Rübe CE, et al. Protecting the heritable genome: DNA damage response mechanisms in spermatogonial stem cells. DNA Repair (Amst) 2011;10(2):159–68.
[34] Cornelissen B, et al. Imaging DNA damage in vivo using gammaH2AX-targeted immunoconjugates. Cancer Res 2011;71(13):4539–49.
[35] Polak JM, et al. Introduction to immunocytochemistry. 2nd ed. Oxford (UK): BIOS Scientific Publishers Ltd.; 1997. ISBN: 1-85996-086-3.
[36] Berkovich E, et al. Roles of ATM and NBS1 in chromatin structure modulation and DNA double-strand break repair. Nat Cell Biol 2007;9(6):683–90.
[37] Iijima K, et al. Dancing on damaged chromatin: functions of ATM and the RAD50/MRE11/NBS1 complex in cellular responses to DNA damage. J Radiat Res 2008;49(5):451–64.
[38] Burma S, et al. ATM phosphorylates histone H2AX in response to DNA double-strand breaks. J Biol Chem 2001;276(45):42462–7.
[39] Takahashi A, et al. ATM is the predominant kinase involved in the phosphorylation of histone H2AX after heating. J Radiat Res 2010;51(4):417–22.
[40] Stiff T, et al. ATM and DNA-PK function redundantly to phosphorylate H2AX after exposure to ionizing radiation. Cancer Res 2004;64(7):2390–6.
[41] Wang H, et al. Complex H2AX phosphorylation patterns by multiple kinases including ATM and DNA-PK in human cells exposed to ionizing radiation and treated with kinase inhibitors. J Cell Physiol 2005;202(2):492–502.
[42] Goodarzi AA, et al. The influence of heterochromatin on DNA double strand break repair: getting the strong, silent type to relax. DNA Repair (Amst) 2010;9(12):1273–82.
[43] Kill IR. Localisation of the Ki-67 antigen within the nucleolus. Evidence for a fibrillarin-deficient region of the dense fibrillar component. J Cell Sci 1996;109(6):1253–63.
[44] Ghule PN, et al. Cell cycle dependent phosphorylation and subnuclear organization of the histone gene regulator p220(NPAT) in human embryonic stem cells. J Cell Physiol 2007;213(1):9–17.
[45] Golfier S, et al. Dicentric chromosomes and gamma-H2AX foci formation in lymphocytes of human blood samples exposed to a CT scanner: a direct comparison of dose response relationships. Radiat Prot Dosimetry 2009;134(1):55–61.
[46] Beels L, et al. gamma-H2AX foci as a biomarker for patient X-ray exposure in pediatric cardiac catheterization: are we underestimating radiation risks? Circulation 2009;120(19):1903–9.
[47] Viau M, et al. Global quantification of γH2AX as a triage tool for the rapid estimation of received dose in the event of accidental radiation exposure. Mutat Res Genet Toxicol Environ Mutagen 2015;793:123–31.
[48] Kroeber J, et al. Distinct increased outliers among 136 rectal cancer patients assessed by γH2AX. Radiat Oncol 2015;10:36.
[49] Wang LH, et al. Monitoring drug-induced gammaH2AX as a pharmacodynamic biomarker in individual circulating tumor cells. Clin Cancer Res 2010;16(3):1073–84.
[50] Ivashkevich A, et al. Use of the γ-H2AX assay to monitor DNA damage and repair in translational cancer research. Cancer Lett 2012;327(1–2):123–33.
[51] de Lapuente J, et al. The Comet Assay and its applications in the field of ecotoxicology: a mature tool that continues to expand its perspectives. Front Genet 2015;6:180.
[52] Shaposhnikov S, et al. Fluorescent in situ hybridization on comets: FISH comet. Methods Mol Biol 2015;1288:363–73.
[53] Cortés-Gutiérrez EI. Interpreting sperm DNA damage in a diverse range of mammalian sperm by means of the two-tailed comet assay. Front Genet 2014;5:404.
[54] Spivak G. The Comet-FISH assay for the analysis of DNA damage and repair. Methods Mol Biol 2010;659:129–45.
[55] Spivak G, et al. New applications of the Comet assay: comet-FISH and transcription-coupled DNA repair. Mutat Res 2009;681(1):44–50.
[56] Glei M, et al. Analysis of DNA damage and repair by comet fluorescence in situ hybridization (Comet-FISH). Methods Mol Biol 2014;1094:39–48.
[57] McKenna DJ. Use of the comet-FISH assay to compare DNA damage and repair in p53 and hTERT genes following ionizing radiation. PLoS One 2012;7(11):e49364.
[58] Guo J. Comet-FISH with strand-specific probes reveals transcription-coupled repair of 8-oxoGuanine in human cells. Nucleic Acids Res 2013;41(16):7700–12.
[59] Zeljezic D, et al. Evaluation of genome damage in subjects occupationally exposed to possible carcinogens. Toxicol Ind Health 2015. pii:0748233714568478, [in press].
[60] Pérez-García C, et al. Development of a comet-FISH assay for the detection of DNA damage in hemocytes of *Crassostrea gigas*. Aquat Toxicol 2015;161:189–95.
[61] Mori T, et al. Simultaneous establishment of monoclonal antibodies specific for either cyclobutane pyrimidine dimer or (6-4) photoproduct from the same mouse immunized with ultraviolet-irradiated DNA. Photochem Photobiol 1991;54(2):225–32.
[62] Perdiz D, et al. Distribution and repair of bipyrimidine photoproducts in solar UV-irradiated mammalian cells. Possible role of Dewar photoproducts in solar mutagenesis. J Biol Chem 2000;275(35):26732–42.
[63] Nikitaki Z, et al. Stress-induced DNA damage biomarkers: applications and limitations. Front Chem 2015;3:35.
[64] Choi JH, et al. Highly specific and sensitive method for measuring nucleotide excision repair kinetics of ultraviolet photoproducts in human cells. Nucleic Acids Res 2014;42(4):e29.
[65] Bowman KK, et al. Excision-repair patch lengths are similar for transcription-coupled repair and global genome repair in UV-irradiated human cells. Mutat Res 1997;385(2):95–105.

[66] Hanawalt PC. Controlling the efficiency of excision repair. Mutat Res 2001;485(1):3–13.
[67] Hoeijmakers JH. Genome maintenance mechanisms for preventing cancer. Nature 2001;411(6835):366–74.
[68] Wood RD. DNA damage recognition during nucleotide excision repair in mammalian cells. Biochimie 1999;81(1–2):39–44.
[69] Svetlova M, et al. Clustered sites of DNA repair synthesis during early nucleotide excision repair in ultraviolet light-irradiated quiescent human fibroblasts. Exp Cell Res 2002;276(2):284–95.
[70] Solovjeva L, et al. Differential incorporation of halogenated deoxyuridines during UV-induced DNA repair synthesis in human cells. DNA Repair (Amst) 2005;4(3):359–66.
[71] Madsen P, et al. S-phase patterns of cyclin (PCNA) antigen staining resemble topographical patterns of DNA synthesis. A role for cyclin in DNA replication? FEBS Lett 1985;193(1):5–11.
[72] Celis JE, et al. Increased nuclear cyclin/PCNA antigen staining of non S-phase transformed human amnion cells engaged in nucleotide excision DNA repair. FEBS Lett 1986;209(2):277–83.
[73] Svetlova M, et al. Reduced extractability of the XPA DNA repair protein in ultraviolet light-irradiated mammalian cells. FEBS Lett 1999;463 (1–2):49–52.
[74] Volker M, et al. Sequential assembly of the nucleotide excision repair factors in vivo. Mol Cell 2001;8(1):213–24.
[75] Wakasugi M, et al. DDB accumulates at DNA damage sites immediately after UV irradiation and directly stimulates nucleotide excision repair. J Biol Chem 2002;277(3):1637–40.
[76] Halicka HD, et al. Histone H2AX phosphorylation after cell irradiation with UV-B: relationship to cell cycle phase and induction of apoptosis. Cell Cycle 2005;4(2):339–45.
[77] Moné MJ, et al. Local UV-induced DNA damage in cell nuclei results in local transcription inhibition. EMBO Rep 2001;2(11):1013–7.
[78] Ward IM, et al. Histone H2AX is phosphorylated in an ATR-dependent manner in response to replicational stress. J Biol Chem 2001;276(51): 47759–62.
[79] Marti TM, et al. H2AX phosphorylation within the G1 phase after UV irradiation depends on nucleotide excision repair and not DNA double-strand breaks. Proc Natl Acad Sci USA 2006;103(26):9891–6.
[80] Hanasoge S, et al. H2AX phosphorylation after UV irradiation is triggered by DNA repair intermediates and is mediated by the ATR kinase. Carcinogenesis 2007;28(11):2298–304.
[81] Lu C, et al. Cell apoptosis: requirement of H2AX in DNA ladder formation, but not for the activation of caspase-3. Mol Cell 2006;23(1):121–32.
[82] Moser J, et al. The UV-damaged DNA-binding protein mediates efficient targeting of the nucleotide excision repair complex to UV-induced photo lesions. DNA Repair 2005;4(5):571–82.
[83] Treiber DK, et al. An ultraviolet light-damaged DNA recognition protein absent in xeroderma pigmentosum group E cells binds selectively to pyrimidine (6-4) pyrimidone photoproducts. Nucleic Acids Res 1992;20(21):5805–10.
[84] Dreze M, et al. Monitoring repair of UV-induced 6-4-photoproducts with a purified DDB2 protein complex. PLoS One 2014;9(1):e85896.